Journal Pre-proof

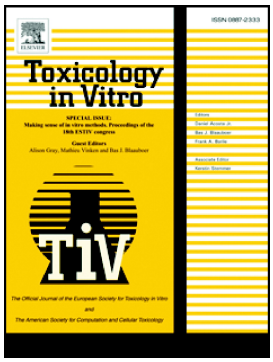

Fluid shear stress affects the metabolic and toxicological response of the rainbow trout gill cell line RTgill-W1

Penelope C. Fenton, Christopher J. Turner, Christer Hogstrand, Nicolas R. Bury

PII: S0887-2333(23)00039-5

DOI: https://doi.org/10.1016/j.tiv.2023.105590

Reference: TIV 105590

To appear in: *Toxicology in Vitro*

Received date: 13 October 2022

Revised date: 20 January 2023

Accepted date: 23 March 2023

Please cite this article as: P.C. Fenton, C.J. Turner, C. Hogstrand, et al., Fluid shear stress affects the metabolic and toxicological response of the rainbow trout gill cell line RTgill-W1, *Toxicology in Vitro* (2023), https://doi.org/10.1016/j.tiv.2023.105590

Fluid shear stress affects the metabolic and toxicological response of the rainbow trout gill cell line RTgill-W1.

Penelope C. Fenton[1], Christopher J. Turner[2], Christer Hogstrand[3] and Nicolas R. Bury[1]

1. University of Southampton, School of Ocean and Earth Science, European Way, Southampton, SO14 3ZH.

2. University of Suffolk, School of Engineering, Arts, Science and Technology, James Hehir Building, University Quays, Ipswich, Suffolk, IP3 0AQ, United Kingdom

3. King's College London, Department of Nutritional Sciences, Franklin Wilkins Building, 150 Stamford Street, London, SE1 9NH, United Kingdom

Key words: Gills, RTgill-W1, Copper toxicity, Fluid shear stress, Mechanosensory

ABSTRACT

The Rainbow trout gill cell-line (RTgill-W1) has been accepted by the Organisation for Economic Co-operation and Development (OECD TG249) as a replacement for fish in acute toxicity tests. In these tests cells are exposed under static conditions. In contrast, in vivo, water moves over fish gills generating fluid shear stress (FSS) that alters cell physiology and response to toxicants. The current study uses a specialised 3D printed chamber designed to house inserts and allows for the flow (0.2 dynes cm^2) of water over the cells. This system was used to assess RTgill-W1 cell responses to FSS in the absence and presence of copper (Cu) over 24h. FSS caused increased gene expression of mechanosensitive channel *peizo1* and the Cu-transporter *atp7a*, elevated reactive oxygen species generation and increased expression of superoxidase dismutase. Cell metabolism was unaffected by Cu (0.163 µM to 2.6 µM Cu) under static conditions but significantly reduced by FSS + Cu above 1.3 µM. Differential expression of metallothionein (*mt*) a and b was observed with increased expression of *mta* under static conditions and *mtb* under FSS on exposure to Cu. These findings highlight toxicologically relevant mechanosensory responses by RTgill-W1 to FSS that may influence toxicological responses.

INTRODUCTION

The rainbow trout gill cell line RTgill-W1 (Bols et al, 1994) has been approved by the Organisation for Economic Co-operation and Development (OECD) as a replacement for fish in acute toxicity testing (OECD TG249). This move meets societal and economical demands for animal free chemical risk assessment by reducing both the cost and the number of animals used in these tests (Hartung, 2017). The cell-based assay uses a suite of cell viability measurements to derive the EC50 (concentration leading to a 50% loss in cell viability) following a static exposure to a chemical. Static conditions allow development of an unstirred layer apical to the cells of approximately 1.6 mm in standard 12 or 24 well culture plates (taken as an average form Hidalgo et al., 1991; Hilgers et al., 1990; Karlsson and Artursson 1991; Shibayama et al., 2015). The layer can become the rate-limiting factor on the permeation of compounds known to enter the cells (Stoker, 1973, Chang et al., 2021). In vivo, the movement of water across the gill reduces the unstirred layer and chemical diffusion distance to approximately 0.036 mm (average from Hughes 1966, Piiper et al., 1986; Shepherd, 1992). Furthermore, water flow elicits fluid shear stress (FSS) on the gill cells in addition to that from the flow of capillary blood on the basolateral surface (Piiper and Scheid, 1984).

In mammals the physiological levels of FSS range from 0.1 dyne/cm^2 for interstitial fluid to > 60 dynes/cm^2 in small arterioles (Ballerman et al., 1998). This force acts as a mechanosensory trigger for several known changes in cellular behaviour, such as increased expression of cell-cell adhesion molecules (Delon et al., 2019), cell polarisation (Jang et al., 2013), altered cytoskeletal arrangement (Flitney et al., 2009), increased membrane fluidity (Haidekker et al., 2000) and gene expression (Snouber et al., 2012). For example, Madin-Darby canine kidney II (MDCKII) cells transport organic cations at increased rates that correlate with rising levels of shear stress and expression of organic cation transporter 2 (*OCT2*) (Jayagopal et al., 2019). With respect to transepithelial resistance (TEER), the intestinal cell line Caco-2 increases expression of cell adhesion molecule zonula occludens

in response to FSS (Delon et al., 2019), and Huh et al. (2010) report increase transepithelial resistance (TEER) in the lung cell line NCI H441 when grown in a biomimetic microsystem that replicates the FSS and alveolar/capillary interface of the human lung. However, there is no correlation between the expression of tight junction genes and increased TEER which is dependent on intensity of FSS and the type of epithelial/endothelial cell model used (Kim et al., 2012: Tan et al., 2018). Morphological changes have also been reported following FSS in Caco-2 cells. Replication of peristaltic intestinal fluid force caused cells to differentiate and develop intestinal villi and basal crypts, and triggered differentiation of mucus-secretory, entero-endocrine and Paneth cells (Kim et al 2012). FSS also influences the toxicological response of cells. In Human umbilical vein endothelial cells (HUVEC) Feng et al (2019) showed increased effectiveness of the cancer drug Vandetanib, which increased apoptosis under low levels of FSS (~ 0.1 dynes/cm^2) when compared to static controls. In addition, Conway et al (2010) reported elevated, expression of the metal binding protein, MT in response to shear stress in vertebrate endothelial cells.

Drieschner et al. (2019) is the only study to use a microfluidic system to assess the effects of FSS of 0.02 dynes/cm^2 on rainbow trout gut cell line TEER. In this study, we expand this observation to other epithelial cells and tested the hypotheses that FSS would alter gene expression of the mechanosensory cation channel *piezo 1*, the TEER and response to Cu of RTgill-W1. The flow rate was set at 20 mL/min based on the lowest measured flow rate of 22 mL/min in resting rainbow trout (Davis and Cameron (1971), which equates to 0.2 dynes/cm^2 of FSS in our chambers. Cu is a vital trace nutrient and cofactor to essential homeostatic enzymes such as antioxidant superoxide dismutase (SOD), yet excess Cu causes cytotoxic build-up of reactive oxygen species (Puig and Thiele, 2002). Intracellular Cu homeostasis is orchestrated through MT, ATPase copper transporting alpha (ATP7A) (Chelly et al., 1993) and antioxidant 1 copper chaperone (ATOX1) (Lin and Culotta, 1995) under normal conditions. However, increases in Cu exposure overwhelm these controls leading to cell damage (Bury et al.,2003).

MATERIALS AND METHODS

Set-up of flow-through system

Flow chambers were designed on Tinkercad (Autodesk, California), to fit 12 or 24 - well cell culture inserts (Falcon) and produced on a desktop 3D printer using acrylonitrile styrene acrylate (ASA) filament (Filamentive, Bradford, UK). The chambers were housed within an autoclavable container and connected to a peristaltic pump (Marlow-Watson, 12-channel) with manifold silicone tubing of 1 mm internal diameter (Fig. 1).

To sterilise the chamber and tubing, the assembled flow system was flushed with 70% industrial methylated spirit (IMS) for 10 minutes. The IMS was drained, and the system rinsed through with sterile L-15/ex [a simplified medium without FBS containing the following constituents (mg/L): $CaCl_2$, 40.0; $MgCl_2$, 93.7; $MgSO_4$, 97.7; KCl, 400.0; KH_2PO_4, 60.0; NaCl, 8000.0; Na_2HPO_4, 190.0; D+ Galactose, 900.0 and Na-Pyruvate, 550.0 (Schirmer et al., 1997)] and drained again. Finally, fresh L-15/ex was added and allowed to flush through for ten minutes before a final draining.

Cell culture

Cell line RTgill-W1 was purchased from ATTC (CRL-2523) and passages between 17 and 30 were used throughout the study. RTgill-W1 were cultured according to OECD TG249 in Leibovitz media (L15) without phenol red (Gibco, 21083027), containing 5% FBS (Sigma Aldrich, F7524) and 0.5% gentamycin (Fisher Scientific, 15750060), at 18 ± 1°C. Media was changed every 5 days and confluent 75 cm^2 flasks (Corning) passaged every 12 days.

The cells were seeded in L15 with FBS at a density of 400,000 cells/mL on inverted 12 or 24-well inserts (Schnell et al 2016). Briefly, inverted inserts were placed in a sterile humidity chamber containing 10 mL of L-15/ex. The insert membrane (0.4 µm pore, 0.9 cm^2 effective growth area, polyethylene terephthalate (PET) membrane (BD Falcon, cat. no. 353180) was

primed with 100 µL L15 with FBS for 30 minutes. The L15 with FBS was aspirated, and each insert seeded with 150 µL of a RTgill-W1 suspension for 24-well and 300 µL for 12-well inserts. A dome of suspended cells was created upon each insert and was left to incubate at 18 ± 2°C for 24 h after which, media on inserts was aspirated and replaced with 150 µL of fresh L15 with FBS. Inserts were left to grow for another 24 h.

Fluid shear stress conditions and exposures

Each box housing (Figure 1) received 2 mL of L-15/ex to maintain a humid atmosphere. Approximately 9 mL of L-15/ex was added to the chamber under flow of 2 mL / min generated by peristaltic pump (Fig. 1) which was calculated according to (Drieschner et al., 2019) as 0.2 dyne / cm^2 ± 0.1 FSS. The chamber and tubing were allowed to fill ensuring removal of trapped air. The seeded inserts were initially washed by placing in a 24-well companion plate (Falcon) containing sterile L15/ex. Insert confluence was checked using an inverted microscope and any non-confluent inserts noted and discarded. One hundred and fifty µL of L15 with 5% FBS was added to the inside of each insert (basolateral to the cell layer).

Cells were exposed to L-15/ex or L-15/ex containing $CuS0_4.5H_2O$ at concentrations of 2.6 µM, 1.3 µM, 0.65 µM, 0.325 µM and 0.163 µM Cu. All concentrations reported refer to nominal Cu concentrations, which equates to free Cu^{2+} concentrations of 2.2 µM, 1.1 µM, 0.55 µM, 0.28 µM and 0.14 µM, respectively calculated using ChemEQL (Eawag, Switzerland). Static controls were set up for the same treatments and both exposures lasted 24 hours and took place at 18 ± 2°C in ambient atmosphere.

Cell visualisation and transepithelial electrical resistance (TEER)

To confirm cellular adherence after exposure to FSS cell layers were stained for actin with a nuclear counterstain. The cell-covered membranes were removed from inserts exposed to either static or FSS conditions in L-15/ex for 24 hours. Each membrane was washed in PBS

and cells fixed with a paraformaldehyde-based solution (10% TritonX-100, sigma and 32% paraformaldehyde in PBS) for 25 minutes. Cells were washed 3 times with 0.1% TritonX-100 in PBS and left in the wash solution for 5 minutes after the final wash step to permeabilise the fixed cells. The membranes were soaked in staining solution containing DAPI (Fisher Scientific) and phalloidin (Alexa Fluor™ 594 conjugate, Thermo Fisher) diluted 1:1000 in PBS for 20 minutes. After 3 washes with PBS, membranes were gently tapped dry and mounted on slides with round cover slips using DAKO permanent mounting media (Agilent Technologies). Cells were visualised at the centre of each membrane with a Zeiss axio-observer with excitation and emission wavelengths of 586 nm:603 nm and 359:457 nm for phalloidin conjugate and DAPI, respectively. Images generated from merging DAPI and phalloidin conjugate channels at 200X magnification.

TEER was measured with the Endohm 12 chamber and Evom2 (World Precision Instruments, Hertfordshire, UK). Following either static or FSS 24 h exposures in L15 with FBS or L-15/ex, cell covered inserts were washed with PBS and placed in the Endohm chamber which was pre-filled with 3 mL L-15/ex to act as an electrolyte. The inserts were filled internally with 1 mL L-15/ex and electrode secured for the resistance reading. Three inserts were used for each condition and each measurement carried out in triplicate with a blank insert serving as negative control.

Measuring cellular metabolic activity

Cell metabolism was assessed using the reduction of resazurin to resorufin by NADH and NADPH following the procedures described in OECD 249 TG. Briefly, after 24h exposures the inserts from the flow chambers were removed into a companion well containing 500 μL PBS. For the static inserts, the exposure media was removed, and both the wells and inserts washed with 500 μL PBS. The PBS was removed, and the cells incubated with 500 μL L-15/ex containing 30 μL resazurin (resazurin sodium salt, Sigma Aldrich, 199303) working

solution (1.5 mg/mL resazurin sodium salt in PBS) and incubated in the dark at 18 ± 1°C for 30 mins on a rotator. Absorbance was measured using the Fluostar Omega (BMG Labtech, Ortenberg, Germany) plate reader set for absorbance of 570 nM (resorufin) and 600 nM (resazurin).

Total RNA extraction and reverse transcription

All FSS and static insert exposures for gene expression analysis were conducted with 12-well tissue culture inserts to increase RNA yield. Cells were exposed to the two lowest concentrations of Cu (0.163 µM and 0.325 µM). Following exposure, the inserts containing the cells were placed in companion wells and washed with 500 µL PBS. PBS was removed and 350 µL of lysis buffer was added to remove cells from inserts and lyse membranes. mRNA was extracted using SurePrep™ TrueTotal™ (Thermo Fisher) plus a DNase (Invitrogen) digestion. RNA fidelity was checked via nanodrop (Thermo Fisher). cDNA was synthesised from extracted mRNA using iScript™ reverse transcription (Bio-rad).

Quantitative PCR.

Primers were designed using primer blast (www.ncbi.nlm.nih.gov) and according to Rainbow trout gene sequences from GenBank (Table 1). Housekeeping genes selected for stability across treatments were ubiquitin and elongation factor beta (*efb*). Selection was confirmed in the reference gene selection utility of the CFX maestro software (Bio-rad) and normalised to both housekeeping genes. QPCR was carried out using iTaq Universal SYBR Green Supermix (Bio-rad). Reaction protocol followed 40 cycles of 95°C for 5 seconds and 59°C for 30 seconds using the CFX connect QPCR machine (Biorad). QPCR relative expression was calculated using $2^{-\Delta\Delta Ct}$ in CFX maestro.

Visualisation of reactive oxygen species

A comparison of ROS production between static and FSS conditions in the absence of Cu was assessed. Confluent inserts were loaded with 5 µM cell permeant 2',7'-

dichlorodihydrofluorescein diacetate (H_2DCFDA, Thermo fisher) in L-15/ex for 90 minutes. The inserts were washed twice with PBS to remove excess dye and exposed to L-15/ex under static and FSS conditions for 2 hours. The purpose of this test was to demonstrate ROS generation in response to FSS. Therefore, shorter exposures were chosen due to the transient nature of ROS generation. After the exposures, the PET membranes were checked for consistent confluence then cut from the inserts using a new scalpel blade and wet mounted onto a microscope slide, face down.

To ensure unbiased analysis of the ROS production a randomisation protocol was developed; Petri dishes where coded and matched to the static and FSS slide mounts which were placed inside. The codes were then hidden with tape, and dishes mixed up by hand. Each chosen Petri dish was coded with another number matched to the photographs taken of the inserts with an inverted microscope (EVOS FL, Invitrogen). Images were captured from the centre of the inserts to avoid areas damaged by the removal process. Microscope settings were the same for each image and for quantification the image colour was inverted, the background removed, and the same threshold set for FSS and corresponding static images. The total area above threshold was assessed using ImageJ software.

Statistical analysis

All experiments were repeated at least 3 times with separate batches of cells. Statistical analysis was carried out using GraphPad Prism (version 8) or Sigmaplot version 13.0. Two-way Anova with Holm-Sidak post-hoc test was performed on log transformed data to assess differences between static and flow cell viability data at the different Cu concentrations. A One-way ANOVA with Tukey's post-hoc test was used to assess difference in gene expression under FSS and static Cu exposures. TEER under FSS and static L-15/ex exposures, static and FSS ROS readings were analysed for differences with Welch's t-test.

RESULTS

Cell adhesion and transepithelial resistance

Cells remained attached to the inserts for the duration of FSS exposures (Fig 2 a, b). There was no significant difference in TEER of cell layers between static and FSS exposed inserts (Fig 2 c).

Cellular metabolic activity

Cu up to a total concentration of 2.6 µM did not affect cell metabolism under static exposure conditions (Fig 3). Cell metabolism decreased under FSS in a dose-dependent manner and was significantly reduced in cells exposed to > 0.163 µM Cu (Fig 3).

Gene expression: Static Vs FSS

The genes encoding the Cu transporter, *atp7a*, the mechanosensory ion channel *piezo1* and antioxidant enzymes *sod1* and *sod2* were significantly upregulated under FSS conditions (Fig. 4). *atp7a* showed a 12.7-fold increase and *piezo1* a 2.7-fold increase under FSS relative to the static L-15/ex control (Fig 4). Increases of 2.1- fold and 1.8-fold of *atox1* and *mtf1* respectively were not significant (Fig 4) and *mta and mtb* were not affected by FSS alone (Fig 4).

Gene expression: Fluid shear stress and Cu exposure

Expression of *mta* was up regulated 31.3-fold by static Cu concentrations of 0.163 µM µM and 11.4-fold by 0.325 µM static Cu (Fig 5 a). Conversely, there was a 36-fold reduction in *mta* expression under 0.163 µM Cu + FSS and more than 50-fold reduction for 0.325 µM Cu under FSS. Differences between static concentrations were highly significant however, differences between extents of downregulation for each concentration under FSS, did not satisfy statistical significance.

Expression *of mtb* was, in contrast to *mta*, upregulated by 0.163 µM and 0.325 µM Cu under FSS by 16.3 and 9.2-fold respectively (Fig 5 b). Static Cu exposures caused little change in

expression with approximately a 2-fold downregulation under both treatment concentrations. Upregulation of *mtf1* was only observed under 0.163 µM static Cu treatment (Fig 5 c) but was downregulated under FSS by 0.163 µM and 0.325 µM respectively.

Upregulation of *atp7a* was observed in all 4 treatments compared to the static L-15/ex control (Fig 5 d). Static 0.163 µM, FSS 0.163 µM and FSS 0.325 µM caused 2.4-fold, 2.8-fold and 2-fold increases in *atp7a* expression, respectively. Differences between the three were not significant. However, there was a 25.4-fold increase in *atp7a* expression under static 0.325 µM Cu treatment.

No significant changes in *atox1* expression were observed under static or FSS treatments of 0.163 µM Cu. Static exposure of 0.325 µM increased *atox1* expression 3.1-fold and 0.325 µM Cu + FSS reduced expression by 2-fold (Fig 5 e).

Reactive oxygen species

FSS exposed cells were above the threshold set in Image J for ROS detection over an average of 34% ± 2.8% of their area, while images of static exposures were 8.4% ± 3.4% over threshold (Fig 6 a). FSS induced increases in ROS were significant when compared to static exposures. Fluorescent H_2DCFDA images show ROS intensity (H_2DCFDA green) (Fig 6 b, c).

DISCUSSION

Cell morphology and TEER in response to fluid shear stress

Epithelial cell lines grown under static conditions on solid or permeable supports often do not demonstrate the morphology or function of native cells in vivo. However, there are examples where culturing cell lines under dynamic conditions such as FSS or membrane stretch to mimic condition at the lung, intestine or kidney has shown changes in cell morphology, physiology and functionality that better mimic the intact tissue (Huh et al., 2010; Kim et al.,

2012; Tan et al., 2018; Delon et al., 2019; Drieschner et al., 2019; Jayagopal et al., 2019). Thus, we hypothesised that flow over cell line RTgill-W1 to induce FSS may alter cellular properties such as an increase in TEER to better reflect that measured in intact and primary gill cell cultures (Schnell et al 2016). FSS did not affect the adhesion of the cells to the inserts (Fig 2a & b) and there was no change in TEER over the 24 hours of FSS compared to static (Fig 2c). The level of FSS may have been insufficient to increase TEER, additional stimulus could be required on the basolateral surface (e.g., capillary blood flow), and or external endocrine stimuli. Alternately, the cells are simply unable to increase TEER in response to FSS.

Gene expression in response to fluid shear stress

Fluid sheer stress without Cu treatment, significantly increased levels of *piezo1*, *atp7a*, (Fig 4) *sod1* and *sod2* expression (Fig 6) compared with static no-Cu treatment expression. Piezo1 upregulation shown in this study agrees with previous work in which shear stress upregulated *Piezo1* in murine osteoblastic cell line MC3T3-E1 (e.g. Song et al., 2020). The mechanism that translates shear stress to *piezo1* upregulation was not investigated in the present study, however, Lee et al (2021) discovered that increased *Piezo1* expression was facilitated through p38 MAP-kinase activity and transcription factor Atf2 binding directly to the *Piezo1* promotor region. Studies in human and animal primary cells and cell lines have demonstrated elevated *Piezo1* RNA correlates to an increase in Piezo1 protein synthesis (Caolo et al., 2020, Zhang et al., 2021). Thus, we infer that an increase in *piezo1* gene expression in the present study relates to an increase *in piezo1* translation.

Ca^{2+} readily permeates gated Piezo1 channels (Ilkan et al., 2017; Gnanasambandam et al., 2015; Kuchel et al., 2021; Lee et al., 2021). For example, a *PIEZO1* knockout in HUAECs greatly inhibited shear stress-induced calcium influx (Wang et al., 2016) and the application of Yoda1, a *PIEZO1* agonist, caused a 170% increase in Ca^{2+} transient influx in human platelets. An elevated number of FSS activated Piezo1 channels (Coste at al., 2012) can

increase intracellular Ca^{2+} (Liao et al., 2021). This rise in cellular $Ca2^{2+}$ has been shown to induce ROS production ~~Cellular, and subsequent mitochondrial calcium overload causes pathological consequences at the cellular level via the opening of the mitochondrial transition pore. This allows movement of small solutes between the mitochondrial matrix and cytosol, resulting in loss of proton gradient and impairment of the electron transport chain (ETC) (Peng and Jou, 2010). ETC impairment causes electron leakage from the cycle prior to complex IV (cytochrome c oxidase) and the generation of ROS~~ (Santulli et al., 2015). It is possible that this was the case in RTGill-W1 under FSS where we observe elevated ROS production and expression of *sod1* and *sod2* in response to FSS (Fig 6). SOD enzymes are known antioxidants whilst *Atp7a*, which was upregulated 30-fold by FSS (Fig 4), has been shown to have an antioxidant role in mouse endothelium where calcium influx causes the transporter to activate extracellular SOD by suppling the Cu cofactors for enzyme activity (Sudhahar et al., 2013). In addition, a study of *Atp7a* knockout mouse embryonic fibroblasts showed increased sensitivity to oxidative stress demonstrating a significant role in this transporter in defence against ROS (Zhu et al., 2017). These findings taken with those in the present study suggest FSS induced oxidative stress in RTgill-W1, and this is likely due to an increase in Ca^{2+} influx through Piezo1.

FSS increases the effect of Cu exposure on metabolic activity

Metabolic activity was not reduced in cells exposed to 0.163 µM to 2.6 µM total Cu under static conditions, but was significantly reduced under FSS and exposure to Cu > 1.3 µM (Fig. 3). In static conditions Bopp et al (2008) showed a reduction in RTGill-W1 cell viability above 5 µM total Cu^{2+} (Bopp et al., 2008) with an EC50 of 29.2 µM Cu^{2+} and Scott et al 2020 showed a drop-in metabolic activity with an EC50 of 3.85 µM total Cu^{2+} following 24 h exposure. In the former study the differences to our observations maybe due to the exposure time (2.5 h) and use of a modified Earle's medium. However, these studies also base their findings on measured Cu^{2+} concentrations, whilst in the current study we report nominal concentrations. Cu may bind to the plastic surfaces of the companion well and

insert and Scott et al (2020) reported a drop of Cu concentrations of 15% over 24h in static conditions. Thus, a caveat in our observation that Cu toxicity is enhanced under FSS (Fig. 3) is the need to confirm the exposure concentration. However, the flow-through chamber is a closed system (Fig. 1) and has a much larger surface area to that of a static chamber and thus the greater potential to absorb Cu in effect reducing the exposure concentration. Thus, we may be underestimating the effect concentration. Alternately, this difference in metabolic activity may be explained by a thinner unstirred layer under FSS when compared to static conditions, enhancing the permeation rate of Cu (Stoker, 1973). Although the cell maintains tight regulation of Cu and prevents a rise in intracellular free Cu^{+} under homeostatic conditions, oxidative environments reduce the Cu binding capacity of MT and allow release of Cu from the MT-Cu complex (Fabisiak et al., 1999). ROS induced by Cu + FSS treatments could reduce cell viability through a combination of disruption to Cu control mechanisms together with FFS induced oxidative stress as demonstrated in the no Cu FSS test (Fig. 6a-c).

Differential gene expression to static and FSS under Cu exposure

At low copper concentrations it is generally accepted that excess intracellular Cu is controlled via high affinity metal binding molecules such as MT (Gudekar et al., 2020). At higher concentrations of Cu, these metal binding proteins become saturated, and synthesis of new MT is unable to cope with the influx thus alternative detoxification processes are required. Such processes involve cellular exocytosis where Cu is passed from ATOX1 to trans Golgi network-associated ATP7A, forming Cu-rich vesicles for transfer to the cell membrane for excretion (Dameron and Harrison, 1998). The gene expression analysis from Cu exposure under static conditions concurs with these hypotheses; at the lower sublethal concentration of 0.163 µM Cu [a value that equates to no effect concentration under FSS (Fig. 3)] there is a greater expression of *mtf1* and *mta*, and at the higher concentration of 0.325 µM Cu [which equates to the lowest no effect concentration under FSS conditions (Fig. 3)], gene expression of *mtf1* and *atp7a* was greater than at 0.163 µM Cu (Fig. 5).

In static conditions, *mtb* gene expression did not change with exposure to Cu, although *mtf1*, a metal transcription factor present in the promoter region of the *mtb* gene, expression increased (Fig. 4 c). This contradicts studies on primary fish gill cells where 0.6 µM Cu induced *mtb* expression (Walker et al 2008). In contrast, a rainbow trout gut cell line showed no significant induction of *mtb* after 24-hour exposures to either 0.3 µM or 0.6 µM Cu compared to L-15/ex controls (Ibrahim et al., 2020). Moreover, Cu uptake via the gills in live fish, was shown to peak and then subside, all within 10 hours of Cu exposure (Kamunde et al., 2002). It may be that after 24-hours of exposure to static, non-toxic concentrations, *mtb* expression in RTgill-W1 has saturated and subsequently vanished. At gene level, rainbow trout *mta* contains two more metal response elements (MRE) than *mtb*, while *mtb* possesses an antioxidant response element (ARE) not seen in *mta* (Zafarullan et al., 190; Olsson et al., 1995; Samson et al., 2001; Bury et al., 2008). Thus, *mtb* may be responding to oxidative stress via the ARE following Cu + FSS exposure rather than directly to Cu and is supported by the observation by Samson et al. (2001) of a functional oxidant responsive element in the rainbow trout *mtb* promoter. The existence of the mechano-sensing transcription factor nuclear factor (erythroid-derived 2)-like (*NRF2*) which is shown to target ARE (Takabe et al., 2011) also supports this hypothesis. Together, these factors may explain the observed absence of static *mtb* response to Cu in this study and the strong response under mechanical stimulus. One could posit that crosstalk between the MRE-targeting transcription factor *mtf1* and the ARE-targeting factor *NRF2*, may facilitate a choreographed MT response to either Cu or FSS or to both. Crosstalk between these two transcription factors has been suggested in previous studies (Jackson et al., 2020). However, further work is required with respect to the response in RTgill-W1.

CONCLUSION

This study shows previously un-reported evidence of physiological responses from RTgill-W1 cells to FSS including altered cellular responses to Cu. The observed decrease in cell

metabolism in RTgill-W1 cells under Cu + FSS (Fig. 3) may simply be explained by a thinner unstirred layer under FSS that would enhance the permeation rate of Cu when compared to static exposure (Stoker, 1973), however measurement of the Cu concentrations is required to confirm that there are no differences in exposure. However, the cellular response to FSS alone suggests a more complex mechanically induced response from the cells that has yet to be elucidated. Upregulation of *piezo1* represents a predictable response to FSS, which is seen in other cell lines (e.g. Caolo et al., 2020; Song et al., 2020; Lee et al., 2021; Zhang et al., 2021). FSS alone induced ROS production and increased the expression of the ROS scavengers *sod1* and *2* (Fig .6) suggesting a stress response to FSS. These Cu-free responses to FFS contribute to the characterisation of the now widely used cell line. FSS in combination with Cu downregulates metal response genes *mtf1 and mta,* and Cu handling genes *atox-1* and *atp7a* at 0.325 µM Cu compared to static Cu of the same concentration, yet upregulated *mtb* gene expression (Fig. 5). Some explanation may lay in the differences in *mta* and *mtb* gene responsive elements where *mtb* possesses an ARE (Zafarullan et al., 190; Olsson et al., 1995; Samson et al., 2001; Bury et al., 2008). In this scenario the induction of ARE and MRE transcription factors results in a greater stimulus of *mtb* expression, however a time-course study covering the early stages of exposure to both Cu and FSS would shed light on any choreographed genetic response and potential cross-talk between these two pathways.

These results demonstrate toxicologically relevant differences in the response of RTgill-W1 to Cu exposures under FSS when compared to static assays. RTgill-W1 use in static toxicity tests, such as the OECD TG249, has been accepted as a surrogate for acute fish toxicity assessment due to a good corelation between in vitro and in vivo toxicity. However, while static RTgill-W1 tests correlate to fish lethality, nominal concentrations of 1.65 µM Cu have been shown to affect gill function and structure in vivo (Heerden et al., 2004). Therefore, alternative dynamic exposures may reflect sub-lethal effects on the gill in vivo and this can be explored in future work. Nonetheless, it is interesting that the addition of a stimulus found

at the gills in vivo, results in a significantly lower effect concentration in RTgill-W1 when compared to static exposures.

REFERENCES

Ballermann, B., Dardik, A., Eng, E. and Liu, A. (1998). Shear stress and the endothelium. *Kidney Int.*, 54, S100-S108.

Bols, N., Barlian, A., Chirino-Trejo, M., Caldwell, S., Goegan, P. And Lee, L. (1994). Development of a cell line from primary cultures of rainbow trout, *Oncorhynchus mykiss* (Walbaum), gills. *J. Fish Dis.*, 17, 601-611.

Bopp, S., Abicht, H. and Knauer, K. (2008). Copper-induced oxidative stress in rainbow trout gill cells. *Aquat. Toxicol.*, 86, 197-204.

Bury, N., Walker, P. and Glover, C. (2003). Nutritive metal uptake in teleost fish. Journal of Experimental Biology, 206, 11-23.

Bury, N., Chung, M., Sturm, A., Walker, P. and Hogstrand, C. (2008). Cortisol stimulates the zinc signaling pathway and expression of metallothioneins and ZnT1 in rainbow trout gill epithelial cells. *Am. J. Physiol.*, 294, R623-R629.

Caolo, V., Debant, M., Endesh, N., Futers, T., Lichtenstein, L., Bartoli, F., Parsonage, G., Jones, E. and Beech, D. (2020). Shear stress activates ADAM10 sheddase to regulate Notch1 via the Piezo1 force sensor in endothelial cells. *eLife*, 9, e50684.

Chelly, J., Tümer, Z., Tønnesen, T., Petterson, A., Ishikawa-Brush, Y., Tommerup, N., Horn, N. and Monaco, A. (1993). Isolation of a candidate gene for Menkes disease that encodes a potential heavy metal binding protein. *Nat. Genet.* 3, 14-19.

Conway, D., Lee, S., Eskin, S., Shah, A., Ho, H. and McIntire, L. (2010). Endothelial metallothionein expression and intracellular free zinc levels are regulated by shear stress. *Am. J. Physiol.*, 299, C1461-C1467.

Coste, B., Xiao, B., Santos, J., Syeda, R., Grandl, J., Spencer, K., Kim, S., Schmidt, M., Mathur, J., Dubin, A., Montal, M. and Patapoutian, A. (2012). Piezo proteins are pore-forming subunits of mechanically activated channels. *Nature*, 483, 176-181.

Dameron, C. and Harrison, M. (1998). Mechanisms for protection against copper toxicity. *Am. J. Clin. Nutr*. 67, S1091-S1097.

Davis, J.C. and Cameron, J.N. (1971) Water flow and gas exchange at the gills of rainbow trout, *Salmo gairdneri*, *J. Exp.Biol.* 54, 1–18.

Delon, L., Guo, Z., Oszmiana, A., Chien, C., Gibson, R., Prestidge, C. and Thierry, B. (2019). A systematic investigation of the effect of the fluid shear stress on Caco-2 cells towards the optimization of epithelial organ-on-chip models. *Biomaterials*, 225, 119521.

Drieschner, C., Könemann, S., Renaud, P. and Schirmer, K. (2019). Fish-gut-on-chip: development of a microfluidic bioreactor to study the role of the fish intestine in vitro. *Lab on a Chip*, 19, 3268-3276.

Fabisiak, J., Tyurin, V., Tyurina, Y., Borisenko, G., Korotaeva, A., Pitt, B., Lazo, J. and Kagan, V. (1999). Redox regulation of copper–metallothionein. *Arch. Biochem. Biophy.*, 363, 171-181.

Feng, S., Mao, S., Zhang, Q., Li, W. and Lin, J. (2019). Online analysis of drug toxicity to cells with shear stress on an integrated microfluidic chip. *ACS Sensors*, 4, 521-527.

Flitney, E., Kuczmarski, E., Adam, S. and Goldman, R. (2009). Insights into the mechanical properties of epithelial cells: the effects of shear stress on the assembly and remodeling of keratin intermediate filaments. *FASEB J.*, 23, 2110-2119.

Gnanasambandam, R., Bae, C., Gottlieb, P. and Sachs, F. (2015). Ionic selectivity and permeation properties of human PIEZO1 channels. *PLOS ONE*, 10, e0125503.

Gudekar, N., Shanbhag, V., Wang, Y., Ralle, M., Weisman, G. and Petris, M. (2020). Metallothioneins regulate ATP7A trafficking and control cell viability during copper deficiency and excess. *Sci. Rep.*, 10, 7856.

Haidekker, M., L'Heureux, N. and Frangos, J., (2000). Fluid shear stress increases membrane fluidity in endothelial cells: a study with DCVJ fluorescence. *Am. J. Physiol.*, 278, H1401-H1406.

Hartung, T. (2017). Evolution of toxicological science: the need for change. *Int. J. Risk Assessment and Management*, 20, 21 - 45.

Heerden, D., Vosloo, A. and Nikinmaa, M., (2004). Effects of short-term copper exposure on gill structure, metallothionein and hypoxia-inducible factor-1α (HIF-1α) levels in rainbow trout (Oncorhynchus mykiss). *Aquatic Toxicology*, 69, 271-280

Hidalgo, I.J., Hillgren, K.M., Grass, G.M., and Borchardt, R.T. (1991). Characterization of the unstirred water layer in Caco-2 cell monolayers using a novel diffusion apparatus. *Pharm. Res*. 8, 222-227.

Hilgers, A.R., Conradi, R.A., and Burton, P.S. (1990) Caco-2 cell monolayers as a model for drug transport across the intestinal mucosa. *Pharm. Res*. 7, 902–910.

Hughes, G.M. (1966) The dimensions of fish gills in relation to their function. *J. Exp. Biol*. 45, 177 - 195.

Ilkan, Z., Wright, J., Goodall, A., Gibbins, J., Jones, C. and Mahaut-Smith, M. (2017). Evidence for shear-mediated Ca^{2+} entry through mechanosensitive cation channels in human platelets and a megakaryocytic cell line. *J. Biol. Chem.*, 292, 9204-9217.

Jackson, A., Liu, J., Vallanat, B., Jones, C., Nelms, M., Patlewicz, G. and Corton, J. (2020). Identification of novel activators of the metal responsive transcription factor (MTF-1) using a gene expression biomarker in a microarray compendium. *Metallomics*, 12, 1400-1415.

Jang, K., Mehr, A., Hamilton, G., McPartlin, L., Chung, S., Suh, K. and Ingber, D. (2013). Human kidney proximal tubule-on-a-chip for drug transport and nephrotoxicity assessment. *Integrat. Biol.*, 5, 1119-1129.

Jarsjö, J., Andersson-Sköld, Y., Fröberg, M., Pietroń, J., Borgström, R., Löv, Å. and Kleja, D. (2020). Projecting impacts of climate change on metal mobilization at contaminated sites: Controls by the groundwater level. *Sci. Total Environ.*, 712, 135560.

Jayagopal, A., Brakeman, P., Soler, P., Ferrell, N., Fissell, W., Kroetz, D. and Roy, S. (2019). Apical shear stress enhanced organic cation transport in human OCT2/MATE1-

transfected Madin-Darby canine kidney cells involves ciliary sensing. *J. Pharmacol. Exp. Ther*., 369, 523-530.

Karlsson, J., and Artursson, P. (1991). A method for the determination of cellular permeability coefficients and aqueous boundary layer thickness in monolayers of intestinal epithelial (Caco-2) cells grown in permeable filter chambers. *Int. J. Pharm*. 71, 55-64.

Kim, H., Huh, D., Hamilton, G. and Ingber, D. (2012). Human gut-on-a-chip inhabited by microbial flora that experiences intestinal peristalsis-like motions and flow. *Lab on a Chip*, 12, 2165 - 2174.

Kuchel, P., Romanenko, K., Shishmarev, D., Galvosas, P. and Cox, C. (2021). Enhanced Ca^{2+} influx in mechanically distorted erythrocytes measured with 19F nuclear magnetic resonance spectroscopy. *Sci. Rep.*, 11, 3749.

Lee, W., Nims, R., Savadipour, A., Zhang, Q., Leddy, H., Liu, F., McNulty, A., Chen, Y., Guilak, F. and Liedtke, W. (2021). Inflammatory signaling sensitizes Piezo1 mechanotransduction in articular chondrocytes as a pathogenic feed-forward mechanism in osteoarthritis. *Proc. Nat. Acad. Sci.*, 118, e2001611118.

Lin, S. and Culotta, V. (1995). The ATX1 gene of Saccharomyces cerevisiae encodes a small metal homeostasis factor that protects cells against reactive oxygen toxicity. *Proc. Nat. Acad. Sci.* 92, 3784-3788.

Morling, K. and Fuchs, S. (2021). Modelling copper emissions from antifouling paints applied on leisure boats into German water bodies. *Environ. Pollut.*, 289, 117961.

OECD 249. Organisation for Economic Co-operation and Development, 2021. Test No. 249: Fish Cell Line Acute Toxicity - The RTGill-W1 cell line assay. Paris: OECD Publishing.

Olsson, P-E., Kling, P., Erkell, L., Kille, P. (1995). Structural and functional analysis of the Rainbow Trout (*Oncorhyncus mykiss*) metallothionein-A gene. *FEBS J*., 230, 344-349

Peng, T. and Jou, M. (2010). Oxidative stress caused by mitochondrial calcium overload. *Ann. N. Y. Acad. Sci*., 1201, 183-188.

Piiper, J., Scheid, P., Perry, S.F., and Hughes, G.M. (1986). Effective and morphometric oxygen-diffusing capacity of the gills of the elasmobranch *Scyliorhimus stallaris*. *J. Exp. Biol.* 123, 27-41

Puig, S. and Thiele, D. 2002. Molecular mechanisms of copper uptake and distribution. *Curr. Opin. Chem. Biol*., 6, 171-180.

Samson, S.L., Paramchuk, W.J., Gedamu, L. (2001). The rainbow trout metallothionein-B gene promoter: contributions of distal promoter elements to metal and oxidant regulation. *Biochim. Biophys. Acta*, 1517, 202-211.

Santulli, G., Xie, W., Reiken, S. and Marks, A. (2015). Mitochondrial calcium overload is a key determinant in heart failure. *Proc. Nat. Acad. Sci*., 112, 11389-11394.

Scott, J., Beldon, J.B., Minghetti, M. (2020). Toxicity testing: In vitro-in vivo corelation and optimization of exposure conditions. *Environ. Toxicol., Chem*., 40, 1050 – 1061.

Shepherd, K.L. (1993) Mucus on the epidermis of fish and its influence on drug delivery. *Adv. Drug Del. Rev.* 11, 403–417

Shibayama, T., Morales, M., Zhang, X., Martinez,L., Berteloot, A., Secomb, T.W., Wright, S.H. (2015). Unstirred water layers and the kinetics of organic cation transport. *Pharm. Res.* 32, 2937–2949

Snouber, L., Letourneur, F., Chafey, P., Broussard, C., Monge, M., Legallais, C. and Leclerc, E. (2011). Analysis of transcriptomic and proteomic profiles demonstrates improved Madin-Darby canine kidney cell function in a renal microfluidic biochip. *Biotech. Prog*., 28, 474-484.

Song, J., Liu, L., Lv, L., Hu, S., Tariq, A., Wang, W. and Dang, Y. (2020). Fluid shear stress induces Runx-2 expression via upregulation of PIEZO1 in MC3T3-E1 cells. *Cell Biol. Int*., 44, 1491-1502.

Stoker, M. (1973). Role of diffusion boundary layer in contact inhibition of growth. *Nature*, 246, 200-203.

Sudhahar, V., Urao, N., Oshikawa, J., McKinney, R., Llanos, R., Mercer, J., Ushio-Fukai, M. and Fukai, T. 2013. Copper transporter ATP7A protects against endothelial dysfunction in type-1 diabetic mice by regulating extracellular superoxide dismutase. *Diabetes*, 62, 3839-3850.

Takabe, W., Warabi, E. and Noguchi, N. 2011. Anti-atherogenic effect of laminar shear stress via Nrf2 activation. *Antioxid. Redox Signal*., 15, 1415-1426.

Tan, H., Trier, S., Rahbek, U., Dufva, M., Kutter, J. and Andresen, T. (2018). A multi-chamber microfluidic intestinal barrier model using Caco-2 cells for drug transport studies. *PLOS ONE*, 13, e0197101.

Walker, P., Bury, N. and Hogstrand, C. (2007). Influence of culture conditions on metal-induced responses in a cultured Rainbow trout gill epithelium. *Environ. Sci. Technol*., 41, 6505-6513.

Wang, S., Chennupati, R., Kaur, H., Iring, A., Wettschureck, N. and Offermanns, S. (2016). Endothelial cation channel PIEZO1 controls blood pressure by mediating flow-induced ATP release. *J. Clin. Invest*., 126, 4527-4536.

Zafarullah, M., Olsson, P-E., Gedamu, L. (1990). Differential regulation of metallothionein genes in rainbow trout fibroblasts, RTG-2. *Biochim. Biophys. Acta*, 1049, 318-325

Zhang, Y., Jiang, L., Huang, T., Lu, D., Song, Y., Wang, L. and Gao, J. (2021). Mechanosensitive cation channel Piezo1 contributes to ventilator-induced lung injury by activating RhoA/ROCK1 in rats. *Respir. Res*. 22, 250.

Zhu, S., Shanbhag, V., Wang, Y., Lee, J. and Petris, M. (2017). A role for the ATP7A copper transporter in tumorigenesis and cisplatin resistance. *J. Cancer*, 8, 1952-1958.

Table 1 – Primer sequences used in this study

Gene	Forward	Reverse
Ubiquitin	GAAGCATTCCACCTGATC	GATGAAGGGTGGACTCTTT
Efb	GCTACATCGAGGGGTGGGT	GGTTGTACCAGCGAAGAGCA
Mta	ACACCCAGACAACTACTAC	GGTACAAAAGCTATGCTCAA
Mtb	GCTCTAAAACTGGCTCTTGC	GTCTAGGCTCAAGATGGTAC
mtf1	CCTCTCAGTACGGTCACAGC	CCTGGGACTGGAACTGG
atp7a	CATGCCGGTGACTAAGAAGC	AATGAGGATCCAGGCGAACA
atox1	ATGTGAGGGATGCTCTGGTG	AGCCTCCTTTCCAGTCTTCT
piezo1	AAGAACCGCAATAGTCCGCA	GGTGCGGTCATTCCACTAGA
sod1	TGGTCCTGTGAAGCTGATTG	TTGTCAGCTCCTGCAGTCAC
sod2	TCCCTGACCTGACCTACGAC	GGCCTCCTCCATTAAACCTC

Figure Legends

Fig. 1. **Flow-through system set-up**. 1. The cell culture insert seeded with RTgill-W1 cells on the underside. 2. The insert fits into 3D printed chamber (50 mm X 20 mm X 10 mm) allowing for FSS over the cells (dotted blue line), with static L15 media in the compartment in contact with the insert and basolateral membrane. 3. Two chambers are placed in each sterile housing, containing sterile L-15/ex to maintain humidity. Chambers are connected to a peristaltic pump (4) with sterile silicone tubing. Solid blue lines represent flow through the silicone tubing for two chambers.

Fig. 2. Visualisation of intact RTgill-W1 cell layer and transepithelial resistance. Cells were exposed to L-15/ex under static (a) or fluid shear stress (FSS) conditions (b) for 24 hours. To demonstrate enduring cell attachment after FSS exposure, actin was stained with phalloidin (red) and nuclei counterstained with DAPI. Visualisation was carried out with the Zeiss Axio observer at 200X magnification. (c) TEER measurements under static or FSS conditions, values represent an average of 3 measurements from 3 different batches of cells ± standard deviation. FSS L-15/ex showed no plottable error. No significant differences were found in TEER between static and FSS conditions (Welch's T test).

Fig. 2. Visualisation of RTgill-W1 cells and transepithelial resistance. Cells were exposed to L15/EX under static (a) or fluid shear stress (FSS) conditions (b) for 24 hours. To demonstrate cell attachment after FSS exposure, actin was stained with phalloidin (red) and nuclei counterstained with DAPI. Visualisation was carried out with the Zeiss Axio observer at 200X magnification. (c) TEER measurements under for static or FSS conditions, values represent an average of 3 measurements from 3 different batches of cells ± standard deviation. FSS L-15/ex showed no plottable error. No significant differences were found in TEER between static and FSS conditions (Welch's T test).

Fig. 3. Metabolic activity of RTgill-W1 cells. RT-gill W1 cells were exposed to various concentrations of copper (nominal concentrations, 0.1633, 0.325, 0.65, 1.3, 2.6 µM) under static (circles) and FSS (squares) conditions. Metabolic activity, measured as the reduction of resazurin, was normalised to the respective measurements in static cells receiving no Cu. Values represent the average ± standard deviation of 3 inserts from different batches. Asterisks denote statistical significance between static and flow conditions at each Cu concentration and letter denotes significant difference between the response at the different

Cu concentrations in flow ($p<0.05$, Two-way ANOVA on log-transformed data with a Holm-Sidak post-hoc test). Error bars not shown where standard deviation is in the order of point size.

Fig. 4. Effect of fluid shear stress on gene expression. The expression of *atp7a, peizo-1, atox1, mtf-1, mta* and *mtb* following 24h static (hatched column) or FSS L-15/ex exposure (clear column). Values represent individual inserts from different batches and are expressed relative to the corresponding static batch. The bars represent the average of the 3 values and the asterisks indicate significant difference to the static L-15/ex controls ($p< 0.0001$, Welch's T tests performed on log transformed data).

Fig. 5. Effect of static and fluid shear stress copper exposure on gene expression. The expression of (a) *mta;* (b) *mtb*; (c) *mtf-1*; (d) *atp7a*; (e) *piezo-1* and (f) *atox1* on exposure to 0.163 and 0.325 µM Cu for 24 hrs under static (solid) or FSS (shaded) conditions. Values represent an average of three measurements of three separate exposures ± standard deviation. Values are normalised to the appropriate static or FSS L-15/ex without Cu controls. Asterisks indicate significant differences ($p<0.05$, ** = $p<0.01$, *** = $p<0.001$, **** = $p<0.0001$, one way ANOVA with Tukey's post-hoc test)

Fig. 6. **Reactive oxygen species and superoxide dismutase expression.** (a) Image J particle analysis for ROS in cells following 24 h exposure to L-15/ex under static and (b) FSS conditions. (c) Quantification of ROS detection in static and FSS exposed cells presented as percent of area over set threshold determined by removal of background signal in ImageJ. values are average of images of three separate inserts from three separate exposures. (d) The expression of sod1 and 2 in L-15/ex under FSS expressed relative to static L-15/ex. Values represent average ± standard deviation from 3 separate experiments. Asterisks denote statistical significance (* $p<0.05$, ** $p<0.001$, Welch's T test).

Fig 1

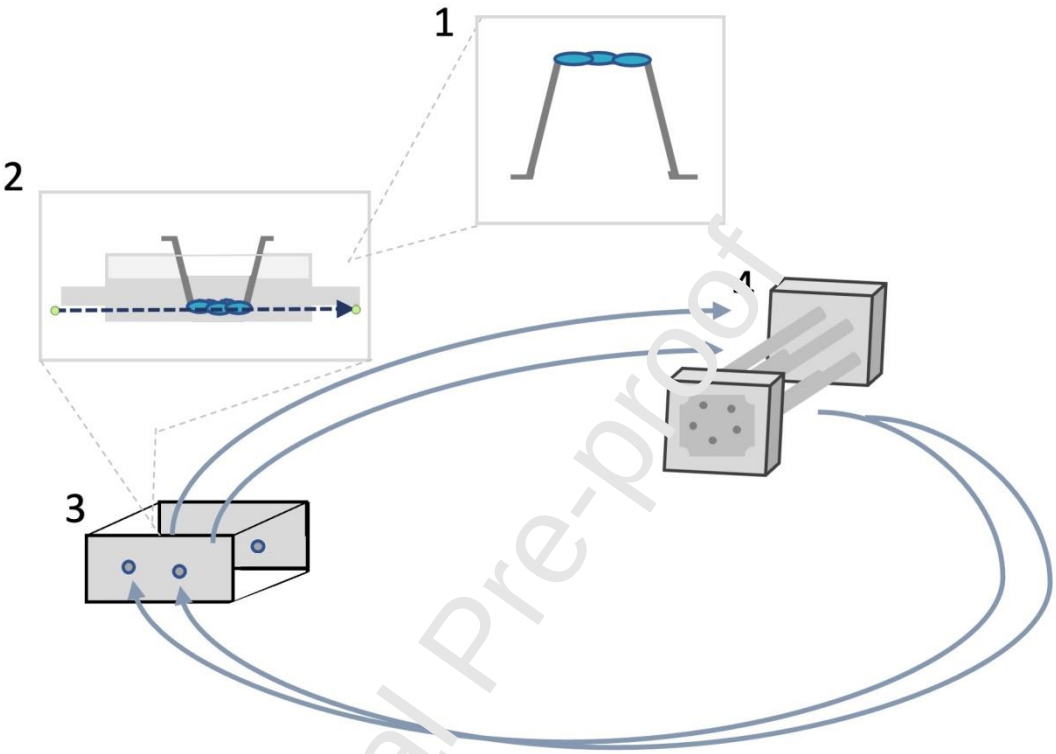

Fig. 2

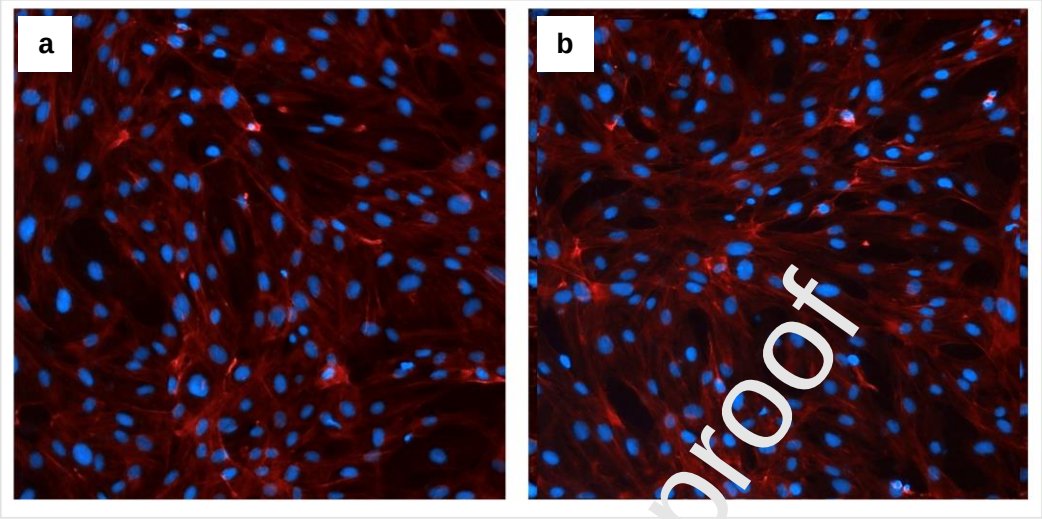

c

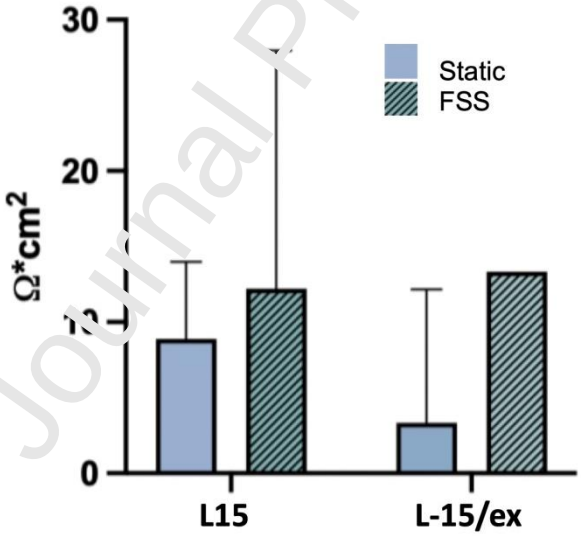

Fig. 3

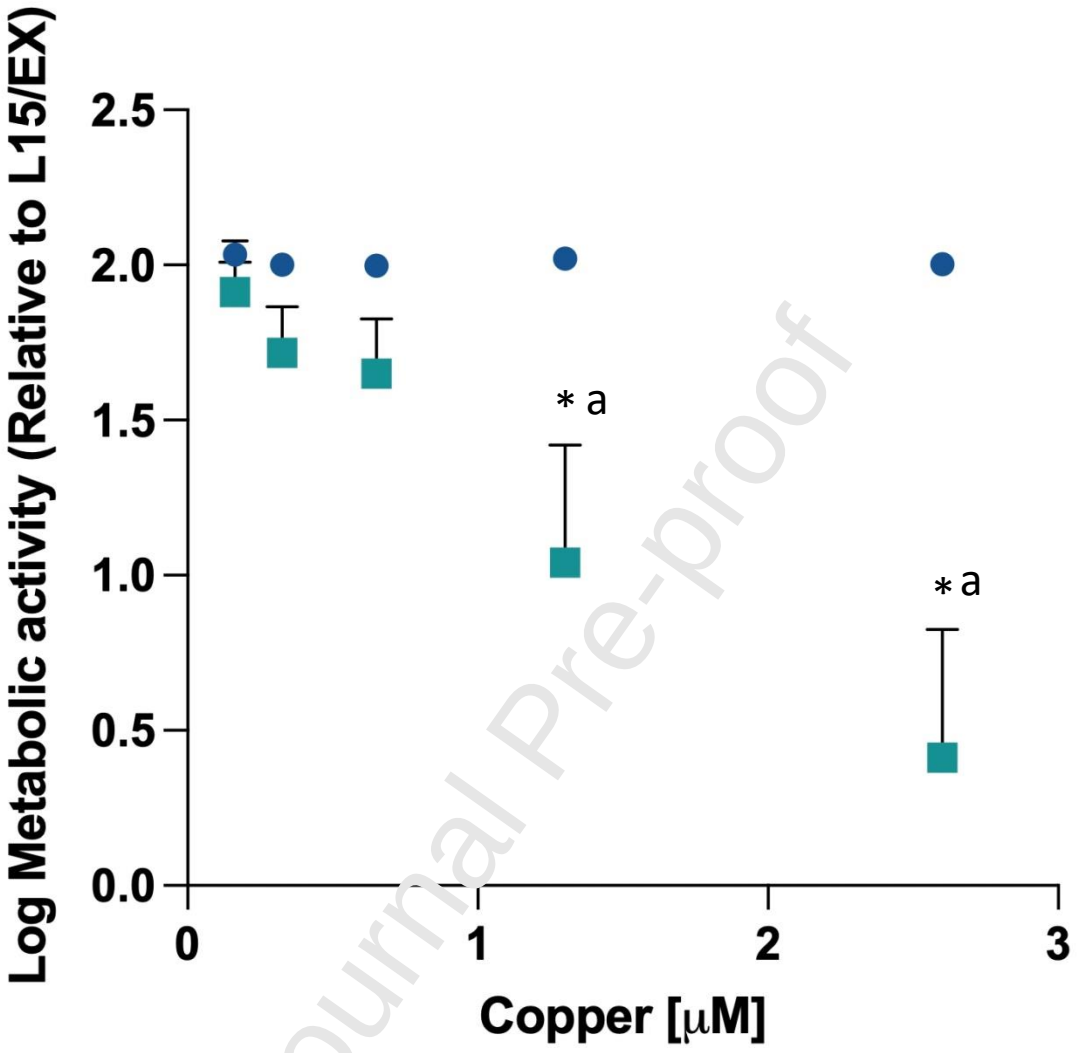

Fig. 4

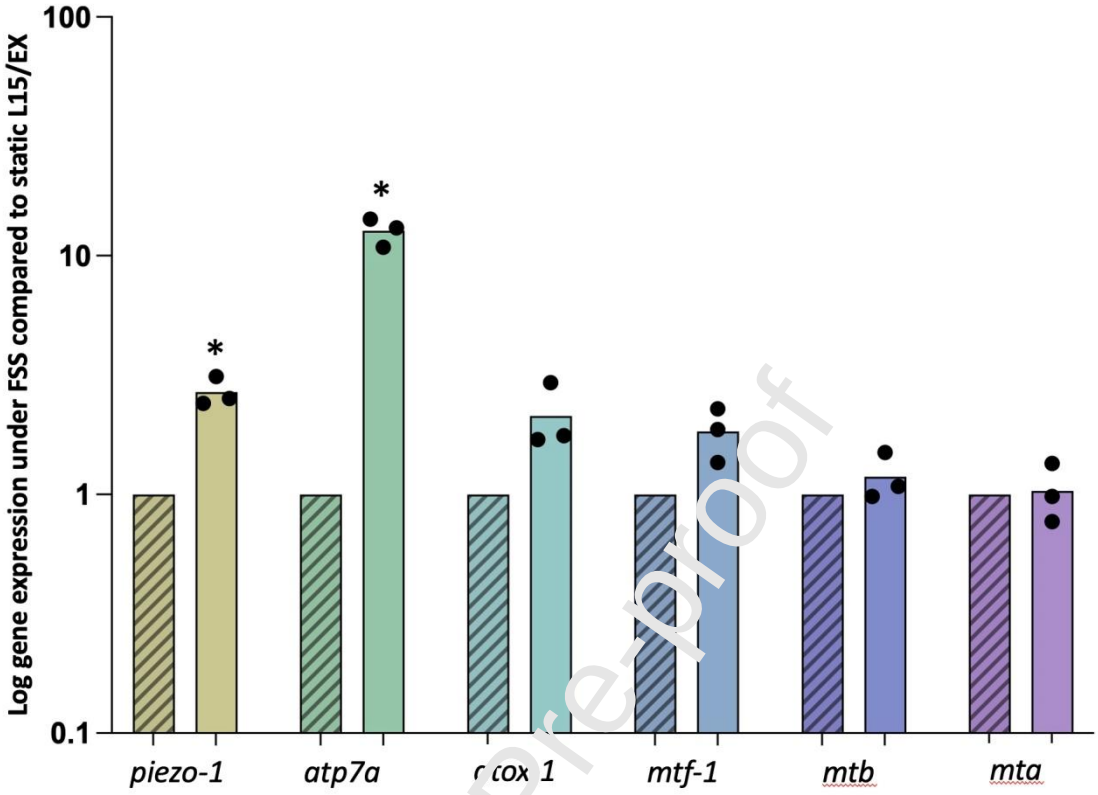

Fig. 5

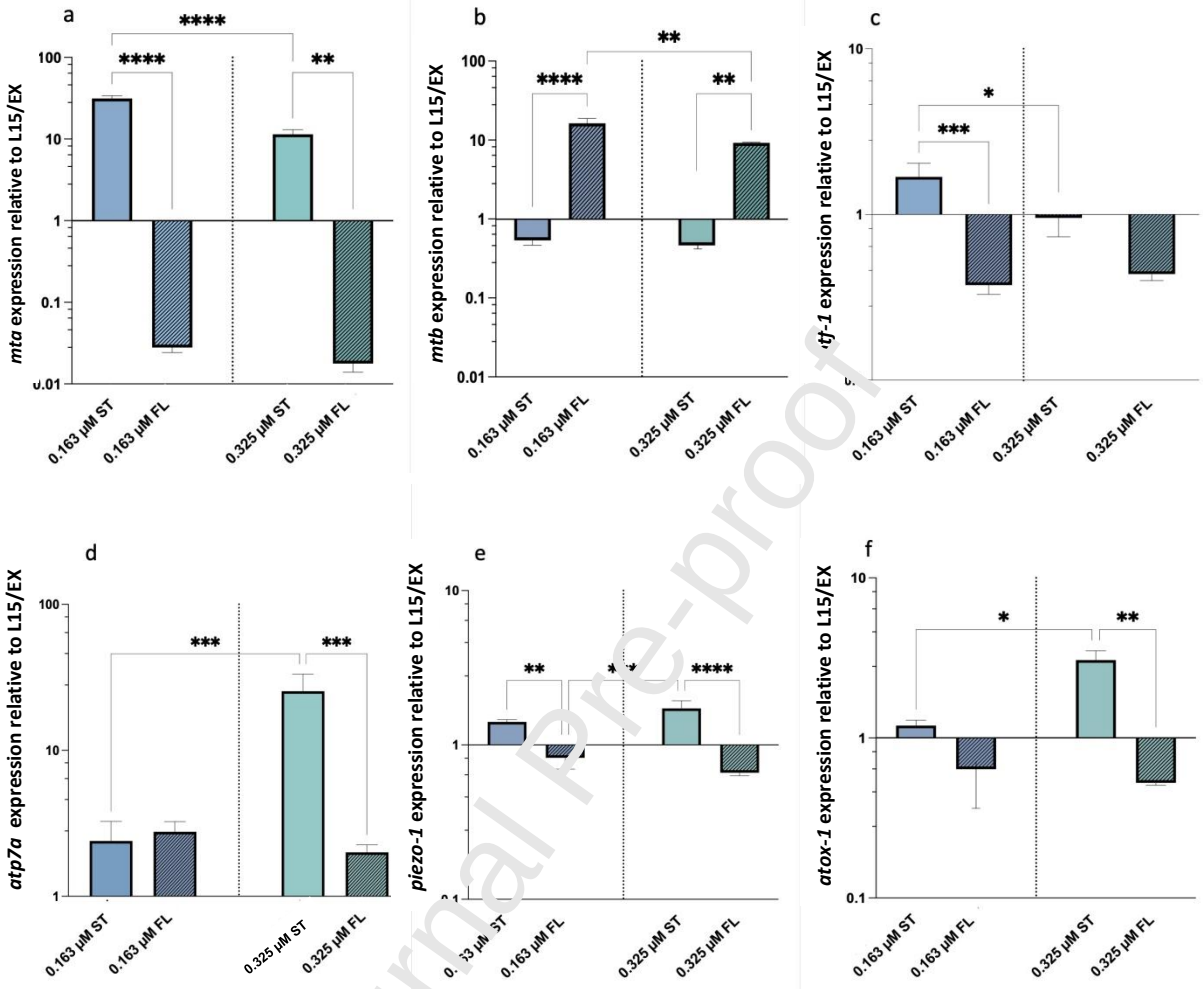

Fig 6.

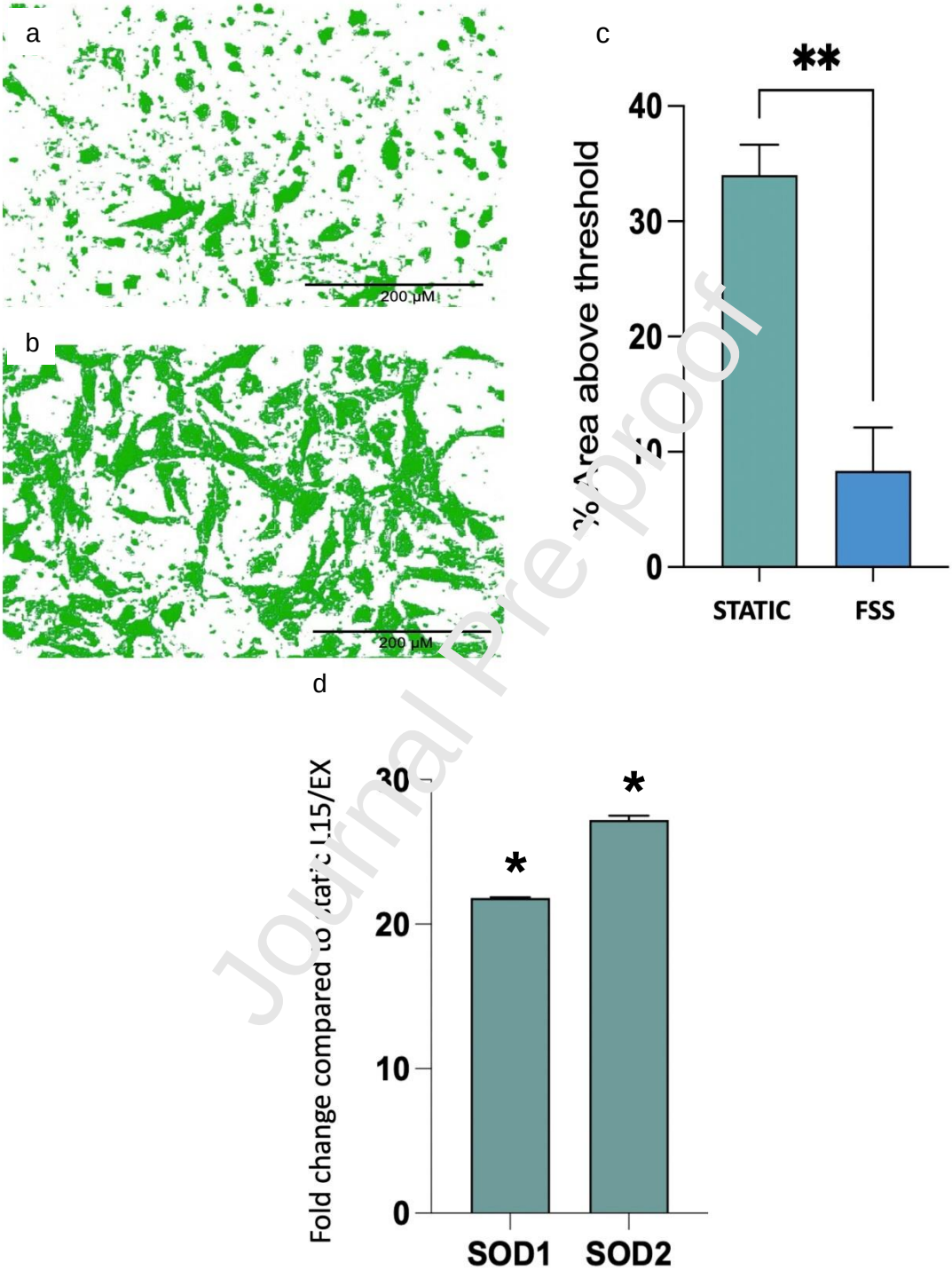

Declaration of interests

☒The authors declare that they have no known competing financial interests or personal relationships that could have appeared to influence the work reported in this paper.

☐The authors declare the following financial interests/personal relationships which may be considered as potential competing interests:

Fluid shear stress affects the metabolic and toxicological response of the rainbow trout gill cell line RTGill-W1.

Penelope Fenton[1], Chris Turner[2], Christer Hogstrand[3] and Nic Bury[1]

Highlights

- Bespoke 3D printed chamber for study of flow on RTgill-W1 cells
- A fluid shear stress of 0.2 dynes cm^{-2} alters gene expression.
- Fluid shear stress reduces the metabolic impact of copper exposure